COMPREHENSIVE CONDITION MONITORING ANALYSIS FOR POWER PLANT BOILER CIRCULATOR PUMPS

Eric Bechhoefer
GPMS Inc
40 Ridge Rd
Cornwall, VT 05753
1 (802) 377-0160
eric@gpms-vt.com

Ed Spence
The Machine Instrumentation Group LLC
4605 Myra Glen Place
Durham, NC 27707
1 (781) 439-1277
ed.spence@machineinstrumentation.com

Abstract: The boiler circulator pump (BCP) is an integral part of the power plant operations in both conventional (coal/gas fired steam plant) or nuclear plants. The BCP moves super heated water under pressure to the steam generator. These pumps are glandless, megawatt induction power pumps. If the pump fails, the power plant must be removed from service to replace the pump. In many applications, these pumps serve power plant providing the base load power requirements of a community. The failure of a pump requires the operator to buy power from other generating plants at much higher rates.

Glandless BCP pose a difficult problem for automated analysis, as there is no way to introduce a tachometer to measure pump speed. Further, while a relatively simple machine, the failure modes include: out of balance/bearing wear that is best measured by vibration, and rotor bar/opens/shorts/eccentricity that is best measured by current. Further, these machines are asynchronous and typically very well balanced, so that is difficult to determine shaft RPM from vibration.

This paper discusses the analysis of BCP using both vibration and current analysis methods and the processing needed to automate fault detection, diagnostics, and prognostics.

Key words: CBM; Diagnostics; Induction Motor; Impact Detection: Rotor Bar;

Introduction: Boiler circulator pumps (BCP) are ubiquitous in steam power generating plants for forced circulation of the working fluid to the steam generator, in both conventional and nuclear facilities. A glandless BCP improves safety and reliability in application where there is high pressure and temperatures for which the uses of a shaft seal is technically, or economically, infeasible.

BCPs designs typically have vertical pumps section suspended from the pipe line without external support. This allows for thermal expansion without distortion or strain on the pump casing. The pump casing is flanged, based on the customer's specification and application. The pump shaft is held in place radially with two water lubricated journal bearings. A tilting pad thrust bearing supports the axial load of the pump hydraulically.

The driving motor and the pump are an integral unit, with the stator and rotor surrounded by water. The water temperature is controlled, typically to 80C, with an auxiliary impeller through a heat exchanger outside of the pump. A thermal heat bearing is provided between the pump and motor section to prevent the heat from the hot pump section to the cooler motor section, thus protecting the motor insulation of the windings. A typical pump is powered by three phase, 4 to 11 KV power of 100 amps and are relatively compact for a MW pump. The capacity of many of these pumps is (depending on head), up to 26,000 gpm, with operating pressures up to 4000+ psi and temperatures of 788F.

The requirement for high availability of power plants coupled with the change in the way these older plants are being operated, give rise to the need for condition monitoring. In the past, coal fired plants were used for base load, with gas fired plants used for peak load. With the low cost of natural gas extraction, gas fired plants are used for base loads, with coal fired plants are being dispatched to supply power for peak loads. A coal fired, base load plant might run for a year without shutting down. Being run to support peak loads, coal fired plants have many more start/stop cycles than they were designed for. As such, BCPs are failing at higher rates and thus have lower reliability. Condition monitoring of BCPs can facilitate opportunistic maintenance and allow for greater flexibility in the operation of a coal-fired plant.

The BCP has a number of wear/damage modes. Electrically, the induction motor can have rotor bar failures, stator winding faults, and dynamic eccentricity. Mechanically, erosion/corrosion over time can cause imbalance. Most concerning is the wear of the journal bearing which will cause whip/whirl or the load of the axial trust bearing due to repeated starts/stops.

A comprehensive condition monitoring system was developed under contract by the pump manufacturer to address the wear/damage modes of the BCP. For the induction motor, both motor current analysis and motor vibration analysis are needed. Current allows for a direct measure of power consumed, rotor bar faults and static/dynamic eccentricity. Vibration allows a measure of the imbalance (shaft order 1), whip/whorl, and a direct measure of slip. To measure a jarring or impact event, continuous monitoring of acceleration is needed. Finally, some capability to measure the direction of rotation could be used. This would afford the ability to check if the power terminal connections were correct.

This paper addresses the analysis the use of a current sensor for motor current analysis, a MEMS smart sensor for vibration analysis, and a MEMS triaxial sensor for impact detection on a BCP.

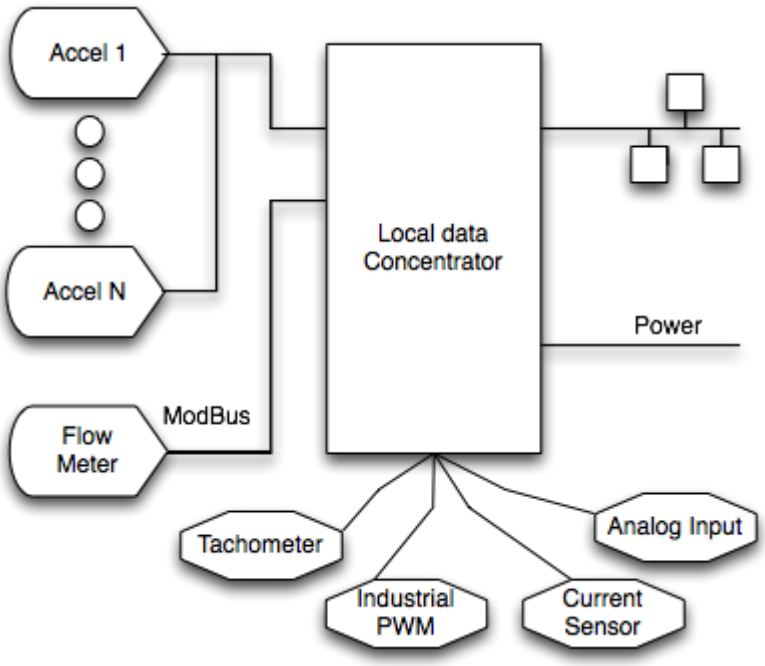

Figure 1 All testing was performed in collaboration with the manufacturer *in situ*, and use the GPMS *Foresight FX* Condition Monitoring System to extract the data, and generate CI's.

Impact Detection: This function requires a duty cycle of 100% as it is never known when an air slug will enter the line, when the pump will be turned off, and if off, when the pump will be energized. Further, the environmental noise is not known, which is needed for threshold setting/impact detection. Finally, direction of the impact force is not know – for example, for a motor start, the force may be tangential or radial, but for a shut down, it might be axial.

The lack of knowledge of the orientation of the sensor, lack of a level of process noise requires a dynamic, self learning system to evaluate what is a valid impact. As such, a tri-axial accelerometer was designed into the onboard control unit (OBCU) which is mounted on the BCP. There are a number of considerations in the design of the system for this implementation.

The design is based on a three channel, tri-axial accelerometer, that uses an initial bias correction at startup. An Alpha tracker then calculates the evolving bias and process noise of the each axis of the tri-axial sensor. The Alpha tracker is related to the Kalman filter, but with the assumption that the plant and process noise do not change. Typically, Kalman filters converge to a steady state relatively quickly. Using this assumption (e.g. that the plant and process noise approach a limit as time approaches infinity), it is possible to define the filter gains, α.

Given the plant noise, σ_w^2 (e.g. now fast the system can change nominally over time) and process noise, σ_v^2 (e.g. the measurement noise of the sensor), the fixed gain for α is calculated as:

$$\lambda = \frac{\sigma_w dt^2}{\sigma_v}, \quad \text{(eq 1)}$$

$$\alpha = {-\lambda^2 + \sqrt{\lambda^4 + 16\lambda^2}}/{8} \quad \text{(eq 2)}$$

During initialization, the bias and process noise σ_v^2, is calculated as:

- For Each Axis (x, y, z)
  - n = n +1
  - delta = x – bias;
  - bias = bias + delta/n;
  - V2 = V2 + delta *(x - bias);
- σ_w^2 = V2/(n-1);

The plant noise represents the "forgetfulness" of the system. Consider that bandwidth (that is, how fast it is anticipated that system could change), may be on the order of 5 minutes, then $\sigma w^2 = 1/(60 * 5)^2$.

The filtered, biased corrected signal, for each axis, is then:

- For each axis, *i*:
  - residual(*i*) = bias(*i*) - measurement(*i*);
  - bias(*i*) = bias(*i*) + α * residual (*i*);

In general the residual(*i*) should have a Gaussian distribution.

Threshold Detection for Shock: There are two potential strategies for detection. If a G limit is know, then a threshold can be set such that the norm vibration level is directly compared to a value, such as 1.0 G. In this case, the norm vibration is:

$$norm = \sqrt{residual_1^2 + residual_2^2 + residual_3^2} \quad \text{(eq 3)}$$

In most cases, this limit is not known. Taking advantage of the assumption that the residual of each measurement from the bias signal is Gaussian, then the sum of the normalized square residuals is a Chi Square statistic with three degrees of freedom. The Chi Square statistic is then:

$$\chi^2 = \left({residual_1}/{\sigma_w}\right)^2 + \left({residual_2}/{\sigma_w}\right)^2 + \left({residual_3}/{\sigma_w}\right)^2 \quad \text{(eq 4)}$$

The threshold is set by taking inverse cumulative distribution function of Chi Square. For a PFA of 10e-6, the threshold is 25.9

The sample rate of each channel was set to 50 Hz, giving a Nyquist of 25 Hz. This is below the 30 Hz shaft rate of the rotor. If the sample rate were higher, the Alpha tracker would need to model the 30 Hz sine wave due to any imbalance on the system.

Motor Analysis: This analysis focuses on the detection of fault relating the drive motor of the pump. While there is a long history of motor analysis (1, 2 and 3), there are few automated systems to report the condition of a motor. Because Motor Current Signature Analysis (MCSA) is ineffective in the detection of journal/fluid bearings (as used in BCP), this system was designed both with a Rogowski Coil (a current transformer used in the MCSA) and two accelerometers (for the upper and lower journal bearings). As such, both MCSA and vibration based motor analysis were implemented. While the analysis is similar, it is felt that using both analysis are synergistic: vibration can supply information that is not available from current analysis (such as slip), and current can supply valuable information not available from vibration alone (e.g. motor amperage).

Vibration can be used to detect motor problems due to the effect of unbalanced magnetic forces. In general, the current in the motor stator produces a rotating magnetic field. Current is produced in the rotor conductors, which is proportional to the difference between the speed of the rotor and the stator magnetic fields. The rotor does not rotate at a synchronous speed, instead "slipping" backwards through the stators' rotating field.

Because the stator synchronous speed is a function of line frequency and the number of pole pairs in the machine, slip is fined per unit as:

$$s = {(RPM_{rotor} - RPM_{stator})}/{RPM_{stator}} \qquad \text{(eq 5)}$$

Typical slip values of 0.01 to 0.02 are not unusual.

Torque is produced from balanced forces on the rotor. If the forces of attraction are not balanced, vibration occurs. This vibration is then the result of current or air gap variances in the motor. The cause of these magnetic vibration are related to:

- The static and/or dynamic air-gap irregularities
- Broken rotor bars or cracked rotor end rings
- Stator faults (open or short of one coil or more of a stator winding)
- Poor/abnormal connections to the stator windings.

Air Gap Eccentricity: When the distance between the rotor and the stator is not uniform, there will be a change in the magnetic flux over time. This will affect both the rate of change of current in the stator, and also exert a periodic force that can be measured with an accelerometer. Formally, this can be the result of either static or dynamic forces. Static eccentricity occurs then the radial air gap is fixed. This could be due to manufacturing error (e.g. the bearing is not centered on the stator), or in the case of a BCP, due to the force of the pump discharge.

For BCP, which use fluid bearings, the force exerted on the shaft from the bearing increases with the reduction in distance to the bearing face. Under normal operations, the reaction to the pump discharge will asymmetrically load the bearing, causing the machine to run eccentrically. As the bearing material wears, the eccentricity will increase.

Dynamic eccentricity occurs when the minimal air gap follows the rotor. This may be due to imbalance phase power.

The change in current caused by the changing magnetic fields results in side band components in both vibration and MCSA, as in (eq. 6):

$$f_e = fR\left((R \pm 1)\left(1 - {}^{s}/_{p}\right) \pm n\right) \quad \text{(eq. 6)}$$

where:

- f_e is the eccentric frequency
- f is the grid frequency
- R is the number of rotor bars
- p is the number of pole pairs and
- n is the odd harmonics values: 1, 3, 5, 7…

For example, with s of 0.011, four pole-pair and 34 rotor bars, 60 Hz, (eq 6) would frequency centered at 564 Hz, with 120 Hz separations for static eccentricity (204, 324, 444, 564, 685, 802 Hz). For dynamic eccentricity, these frequencies are modulated by the shaft rate, approximately 14.85 Hz.

Rotor Bar Faults: A broken rotor bar is typically the result of a broken weld, due to the period mechanical/vibrational loads induced by the changing magnetic flux. The relative motion of the stator magnetic flied and the rotor generates current in the rotor bars. This current produces the motor torque. When a rotor bar cracks/fails, both current in the stator windings and acceleration can be detected at the frequencies in (7):

$$f_{rb} = f\left(k\left(\left(1 - {}^{s}/_{p}\right) \pm s\right)\right) \quad \text{(eq 7)}$$

where:

- f_{rb} is the rotor bar frequency
- f is the grid frequency
- p is the number of pole pairs and
- k is the harmonics values: 1, 2, 3, …

Typically, these sidebands are formed 2x the slip frequency (e.g.. s x f). Figure 1 shows a spectrum of the current, comparing the rotor bar fault frequencies for a nominal motor, with one broken rotor bar and with two broken rotor bars.

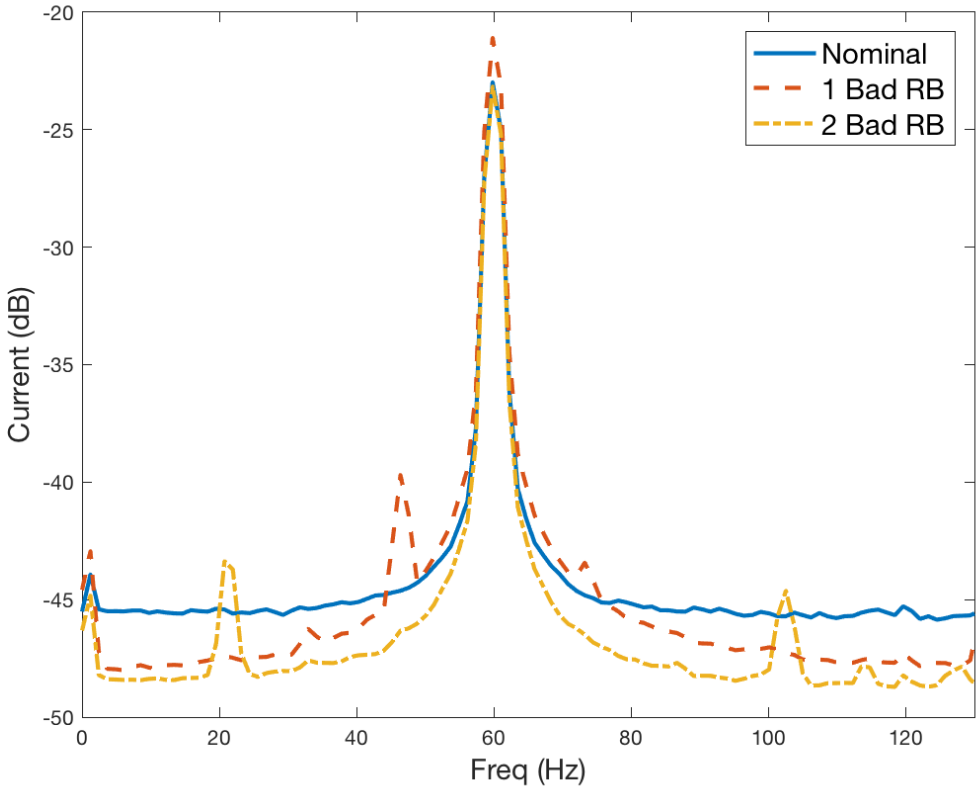

Figure 1. Example of Current Spectrum Comparing Rotor Bar Damage

Note that current clearly shows the fault, but there is little if any indication of what the slip is, especially in the nominal case. The use of vibration allows for a determination of slip simply by measuring the 1/Rev vibration. Figure 2 shows a single phase motor with two broken rotor bars. It is a 4 pole pair design fan, turning nominally at 15 Hz.

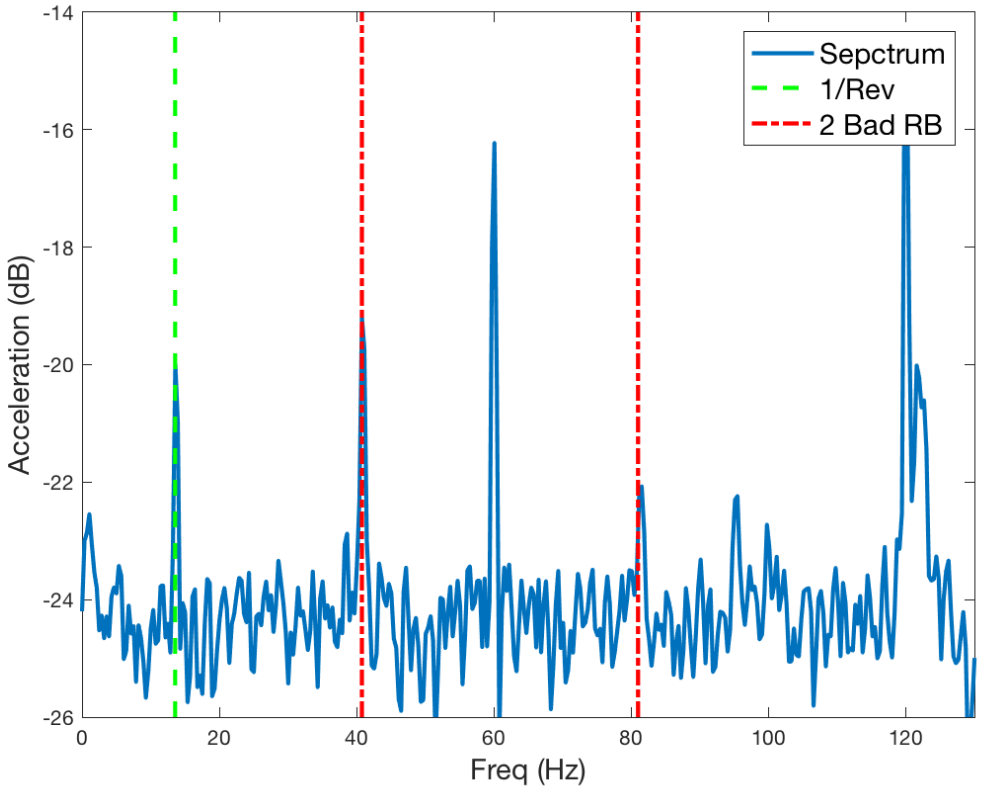

Figure 1. Example of Vibration Spectrum of Fan with Rotor Bar Damage

The measured 1/Rev is 13.56 Hz, giving a large slip of 0.11 – clearly damaged. From (eq 7), sides bands would be expected at [40.22, 52.96, 67.02 and 79.78]. This example shows the side bands at 40.22 and 79.78.

Stator Shorts: Short from turn to turn results in excessive heat and current imbalance. This type of fault typically is not be observed in a BCP, as the working fluid would short the winding to ground rather than a to stator winding. That said, the frequencies associated with MCSA, are in (eq 8).

$$f_s = f\left({}^{n}/_{p}\left((1-s) \pm k\right)\right) \quad \text{(eq 8)}$$

where:

- f_s is the short frequency
- f is the grid frequency
- p is the number of pole pairs and
- k is the harmonic values: 1, 2, 3, …
- n is the harmonic values: 1, 2, 3, …

Note that for vibration analysis, a short, stator looseness, or unbalance phase, etc., is typically seen at 2 x the line frequency.

Mechanical Problems: Many mechanical problems are not well analyzed with current, but are clearly detectable with vibration. Common problems such as imbalance are seen as the 1/Rev (e.g. 1 x RPM) radial vibration. Bent Shaft or Misalignment can be seen in both the radial and axial direction as 1x, and 2x RPM. Bearing faults for rolling element bearings are well documented. The BCP typically uses a fluid bearing, where the damage and wear is associated with whip/whirl (0.43 to 0.48 x RPM).

Rotor Direction: Surprisingly, it rather easy to connect a three-phase motor and have it run in reverse. It is also surprising difficult to determine the direction of rotation of the pump once it is running. As such, there are three indications of a pump running backwards: reduced impeller signature, cavitation and reduced power consumption.

As the pump impeller is designed to run in only one direction, running in reverse causes, as noted, three issues. First, the impeller blades impart a period impulse on the flow of the water which can be measured. Running in reverse, this is much reduced. Second, the pump impeller will generate cavitation when run in reverse, due to a lower pressure on the backside of the impeller. This can be measured as a generalized broadband noise. This noise can be estimated envelope spectrum (e.g. say from 500 to 1000 Hz) as the kurtosis of the spectrum. Increased broadband noise will result in a larger than expected kurtosis at high frequency. The envelope spectrum is used 500 Hz to 1000 Hz, as it is above any of the frequencies that would be expected with the nominal operation of the pump.

As the pump is doing less work (e.g. it is not as effective at moving water) when running in reverse, another indicator is lower power. Measuring motor current is a direct measure of this condition.

Automated Fault Detection: There is a need for automation for fault detection, as most operators do not have the expertise to implement their own condition monitoring program. This requires the automated method to quantify the analysis for specific fault modes on the BCP. This process is exemplified by the generation of condition indicators (CIs), which are then used for component health determination.

CI algorithms implement analysis on the spectrum taken on data. The CI analysis is based on the components being monitoring.

Table 1: Vibration Based Shaft Analysis

Shaft Analysis	Vibration	Comment
SO1 Magnitude	1 x RPM	Unbalance Rotor Shaft
SO2 Magnitude	2 x RPM	Bent Shaft or Angular Misalignment
SO3 Magnitude	3 x RPM	Bent Shaft or Coupling Failure
Impeller	Blades x RPM	Indication of wear/damage to pump/rotation direction
Bearing Analysis	0.43 to 0.48 RPM	Whip/Whirl of fluid bearings
Cavitation	500 to 1000 Hz	Kurtosis of Envelope Spectrum

RPM	Calculated RPM	Pump Status, Used for Slip calculation

Table 2: Vibration Based Motor Analysis

Motor Analysis	Vibration	Comment
Slot Magnitude	# Slots x RPM	Energy Associated the MMF
Short Indicator	2 x Grid Freq	Indication of winding/wind short
Rotor Bar Fault	Eq 7	Sum of Frequency Energies
Rotor Bar Ratio	Eq 7 Normalized	RBF / line frequency energy
Dynamic Eccentricity	Eq 6	Sum of Frequency Energies
Eccentricity Ratio	Eq 6 Normalized	DE / line frequency energy
Slip	Eq 5	Easy to calculate based on vibration

Table 3: Current Based Motor Analysis

Motor Analysis	Current	Comment
Line Amperage	FFT of Line Freq	Magnitude; Pump Condition
Line Frequency	FFT of Line Freq	Calculated Freq.
Slip	Eq 5	Hard to calculate without RBF
Rotor Bar Fault	Eq 7	Sum of Frequency Energies
Rotor Bar Ratio	Eq 7 Normalized	RBF / line frequency energy
Number of Bad RB	Eq 7 Normalized	Log of RBR normalized by line energy
Dynamic Eccentricity	Eq 6	Sum of Frequency Energies
Eccentricity Ratio	Eq 6 Normalized	DE / line frequency energy

Component Health Calculation: While the CI is a used as descriptive statistic of the component under analysis, to be useful, it requires threshold setting. Byington [4] teachers that for single CI, a probability density function (PDF) for the Rician/Rice statistical distribution can be used to set a threshold based on an probability of false alarm (PFA). This was further explored by Dempsey [5], who validated the relationship between CI threshold and PFA to describe the receiver operating characteristics (ROC) of the CI for a given fault. Additionally, Dempsey used the ROC to evaluate the performance of the CI for a fault type. As no single CI has been identified that works with all fault modes, the approached used by Bechhoefer [6] was implemented, which fuses *n* number of CI into a gear health indicator (HI).

Computationally, the use of an HI is attractive. The HI provides a decision making tool for the end user on the status of system health. Health indicators consist of the integration of several condition indicators into one value that provides the health status of the component to the end user [6].

To simplify presentation and knowledge creation for a user, a uniform meaning across all components in the monitored machine was developed. The measured CI statistics (e.g. PDFs) will be unique for each component type (due to different rates, materials, loads, etc). This suggests that the critical values (thresholds) will be different for each monitored component. By using the HI paradigm the HI value is independent of the component. In this implementation, the HI has two alert levels: warning and alarm, allowing a common nomenclature for the HI:

- The HI ranges from 0 to 1, where the probability of exceeding an HI of 0.5 is the PFA,
- A warning alert is generated when the HI is greater than or equal to 0.75. Maintenance should be planned by estimating the RUL until the HI is 1.0.
- An alarm alert is generated when the HI is greater than or equal to 1.0. Continued operations could cause collateral damage.

Note that this nomenclature does not define a probability of failure of the component, or that the component fails when the HI is 1.0. Rather, it represents a reduction in the design reliability of the system and a change in operator behavior to a proactive maintenance policy: perform maintenance to restore the design reliability of the system.

The HI Algorithm: The HI is based on a generalized whitening solution using the Cholesky decomposition (see [7]). The Cholesky decomposition of a Hermitian, positive definite matrix results in:

$$\mathbf{A} = \mathbf{L}\mathbf{L}^{*} \qquad \text{(eq 9)}$$

where **L** is a lower triangular, and $\mathbf{L}^{*}$ is its conjugate transpose. By definition, the inverse covariance is positive definite Hermitian. As such:

$$\mathbf{L}\mathbf{L}^{*} = \mathbf{\Sigma}^{-1}, \text{ and: } \mathbf{Y} = \mathbf{L} \times \mathbf{CI}^{\mathbf{T}}. \qquad \text{(eq 10)}$$

The vector **CI** is the correlated CIs used for the HI calculation, and **Y** is 1 to *n* independent CI with unit variance (one CI representing the trivial case). The Cholesky decomposition, in effect, creates the square root of the inverse covariance. This in turn is analogous to dividing the CI by its standard deviation (the trivial case of one CI). In turn, $\mathbf{Y} = \mathbf{L} \times \mathbf{CI}^{\mathbf{T}}$ creates the necessary independent and identical distributions required to calculate the critical values for a function of distributions.

HI Based on Rayleigh PDFs: The CIs used for this example have Rayleigh like PDFs (e.g. heavily tailed). Consequently, the HI function was designed using the Rayleigh distribution. The PDF for the Rayleigh distribution uses a single parameter, β , resulting in the mean ($\mu = \beta^{*}(\pi/2)^{0.5}$) and variance ($\sigma^2 = (2 - \pi/2) * \beta^2$). The PDF of the Rayleigh is: $x/\beta^2 \exp(x/2\beta^2)$. Note that when applying these equations to the whitening process, the value for β for each CI will then be: $\sigma^2 = 1$, and $\beta = \sigma^2 / (2 - \pi/2)^{0.5} = 1.5264$ (ref [8]).

The HI is then the norm of *n* whitened CIs. As can be show, this function defines a Nakagami PDF [8]. The statistics for the Nakagami are: $\eta = n$ (the number of CIs), and $\omega = 1/(2-\pi/2)*2*n$. The scale value is then calculated from the inverse CDF of the Nakagami for a PFA of 10e-6 at a HI value of 0.5, with η and ω, a

The HI algorithm it then:

$$\boldsymbol{Y} = \boldsymbol{L} \times (\boldsymbol{CI} - \boldsymbol{offset}) \qquad \text{(eq. 10)}$$

$$HI = \sqrt{\boldsymbol{Y}^{T}\boldsymbol{Y}\left(0.5/_{scale}\right)^{2}} \qquad \text{(eq. 11)}$$

The covariance and offset values for the *n* CI were calculated by sampling healthy data from four BCP pumps located at an operators site. This was done by randomly selecting 50 data points from each pump, the calculating the covariance and offsets over the resulting 200 data points. The selected CI's PDF were not Gaussian, but exhibited a high degree of skewness. Because of this, the PDFs were "left shifted" by subtracting an offset such that the PDFs exhibited Rayleigh like distributions.

Deployment: The system has been deployed on four BCP at a coal fired plant. In general, no faults were observed. The Alarm that was observed on a BCP that was undergoing maintenance.

Conclusion: Using an integrated approach to condition monitoring, an attempt was made to build a comprehensive system for monitoring of BCP. Using both accelerometer and current data, analysis was developed to capture all of the fault modes that have been historically observed on BCPs. This integrated approach allows the manufacture of the pump to provided a heighten level of service and reliability to their customer. The pump manufacture is now procuring 22 additional systems for test.

References:

[1] Bates, G. H,. "Vibration Diagnostics for Industrial Electric Motor Drives", Bruel & Kjaer Applications Note, 1980.

[2] Parveenkumar, T., Saimurugan, M., Ramachandran, K. I., "Comparision of Vibraiton, Sound and Motor Current Signature Analysis for Detection of Gear Bos Faults", International Journal of Prognostics and Health Management, 2017

[3] Miljkovic, D., "Brief Review of Motor Current Signature Analysis", Hrčak Portal, Ministry of Science, Education and Sports. 2017.

[4] Byington, C., Safa-Bakhsh, R., Watson., M., Kalgren, P. (2003). *Metrics Evaluation and Tool Development for Health and Usage Monitoring System Technology*. HUMS 2003 Conference, DSTO-GD-0348

[5] Dempsy, P., Keller, J. (2008). Signal Detection Theory Applied to Helicopter Transmissions Diagnostics Thresholds. *NASA Technical Memorandum* 2008-215262

[6] Bechhoefer, E., He, D., (2011). A Process for Data Driven Prognostics, MFPT Publications, Dayton OH

[7] Bechhoefer, E., He, D., Dempsey, P. (2011). *Gear Threshold Setting Based On a Probability of False Alarm*. Annual Conference of the Prognostics and Health Management Society.
[8] Bechhoefer, E., Bernhard, A. (2007). *A Generalized Process for Optimal Threshold Setting in HUMS*. IEEE Aerospace Conference, Big Sky.